Internal Movement in Myosin Subfragment 1 Detected by Fluorescence Resonance Energy Transfer†

Jun Xing and Herbert C. Cheung*

Department of Biochemistry and Molecular Genetics, University of Alabama at Birmingham, Birmingham, Alabama 35294-2041

Received January 25, 1995; Revised Manuscript Received March 15, 1995⊗

ABSTRACT: We have determined intersite distances from Cys374 of actin to Cys707 (SH1) and Cys697 (SH2) of myosin subfragment 1 (S1) in actosubfragment 1 (A·S1) by fluorescence resonance energy transfer for rigor complex A·S1 and complexes containing bound ADP and ADP plus orthovanadate (Vi), A·S1·ADP, and A·S1·ADP·Vi. A single energy acceptor (4-dimethylaminophenylazophenyl-4′-maleimide, DABMI) was attached to Cys374, and two different energy donors [(5-(iodoacetamidoethyl)aminonaphthalene-1-sulfonic acid (IAEDANS) and 2-(4′-maleimidylanilino)naphthalene-6-sulfonic acid (MIANS)] were each attached to SH1 and SH2 for the distance determination. The two sites SH1 and SH2 of S1 were approximately equidistant (ca. 45 Å) from actin Cys374 in rigor A·S1 when MIANS was the energy donor attached to the two thiols. The Cys374−SH1 distance decreased by 7−8 Å in the presence of ADP plus Vi, but the distance Cys374−SH2 was essentially unaltered under identical conditions. Slightly different but similar distance results were obtained with AEDANS as energy donor. If the structure of actin monomer in A·S1 is assumed to be rigid [Miki, M. (1991) *Biochemistry 30,* 10878−10884], the present results indicate that MgADP plus Vi induced a movement of SH1 toward the actin site and that SH2 was insensitive to saturation of the active site pocket of S1 and relatively immobile. These results suggest that during the steady-state hydrolysis of ATP or in the weak-binding state of actomyosin, the short helical segment of S1 heavy chain containing SH1 moves closer to the COOH-terminal end of actin, while the adjacent helical segment containing SH2 remains stationary. The emission spectrum of MIANS attached to SH2 experienced a large red spectral shift (6−10 nm) in the presence of MgADP, MgADP + Vi, MgADP + beryllium fluoride, and ATP. A crude model of S1 based on the C^{α} coordinates suggests that SH2 is located in a hydrophobic cage surrounded by three hydrophobic residues. Reorientation of one of these side chains could expose SH2 to the solvent. The observed red spectral shift of MIANS attached to SH2 could be explained by such a nucleotide-induced exposure, and this explanation would be consistent with the interpretation that SH2 is stationary.

The molecular motor of striated muscle is located in the cross-bridge of the thick filament. This structural element is the subfragment 1 moiety of myosin and contains the sites for interactions with ATP and actin. The binding of ATP to its site in the motor dissociates the cross-bridge from the actin filament and modifies the interaction between myosin and actin, resulting in a "weak" complex between the two proteins. Several elementary steps have been identified or proposed over the years for the hydrolysis of ATP by actomyosin. The release of inorganic phosphate from the substrate pocket of myosin is the rate-determining step of the hydrolysis reaction. This release is accelerated by the reattachment of actin to the cross-bridge, and this step results in a "strong" binding between the two proteins. The actin−myosin interaction alternates rapidly between the two states, dependent upon the absence or presence of bound nucleotide on myosin and the nature of the bound nucleotide (Eisenberg & Greene, 1980; Geeves et al., 1984; Eisenberg & Hill, 1985). The release of inorganic phosphate from myosin is generally regarded as being closely coupled to force generation in muscular contraction. While the structural basis for energy transduction remains unclear, many laboratories have focused on the notion that the transducing element in the motor experiences some kind of global structural changes during ATP hydrolysis and that these changes are related to the transition from the weak-binding state to the strong-binding state. This transition may have a fundamental role in the mechanics of the contractile apparatus.

The strong rigor complexes (myosin·ADP, actin·myosin, actin·myosin·ADP) are stable and their conformations can be readily studied, but the weak complexes (myosin·ATP, myosin·ADP·P_i, actin·myosin·ATP, actin·myosin·ADP·P_i) are short-lived and must be trapped during the ATP cycle for structural studies. A general strategy to stabilize the weak complexes is through cross-linking of two reactive thiols (Cys697 and Cys707) in S1[1] in the presence of ATP or cross-linking of actin with S1, also in the presence of ATP. In these cross-linked species, ATP is stably trapped in the myosin active site pocket. Another approach to generation of stable analogues of myosin·ADP·P_i is substitution of

† This work was supported in part by NIH AR31239.
⊗ Abstract published in *Advance ACS Abstracts,* May 1, 1995.

[1] Abbreviations: S1, myosin subfragment 1; ActoS1; complex formed between actin and S1; A·S1, actoS1; FRET, fluorescence resonance energy transfer; IAEDANS, 5-(iodoacetamidoethyl)aminonaphthalene-1-sulfonic acid; DABMI, 4-dimethylaminophenylazophenyl-4′-maleimide; MIANS, 2-(4′-maleimidylanilino)naphthalene-6-sulfonic acid; FDNB, 2,4-dinitro-1-fluorobenzene; HEPES, 4-(2-hydroxyethyl)-1-piperazineethanesulfonic acid; Tris, tris(hydroxymethyl)-aminomethane; EDTA, ethylenediaminetetraacetic acid; Vi, orthovanadate (VO_4^{3-}); BeF, beryllium fluoride (BeF_3^-); DTT, dithiothreitol.

0006-2960/95/0434-6475$09.00/0

inorganic phosphate with an analogue such as the orthovanadate ion or beryllium fluoride. The stable ternary complex formed by myosin, ADP, and orthovanadate, M^{**}·ADP·Vi, is believed to be a good analogue of the predominant steady-state intermediate M^{**}·ADP·P_i of the magnesium-dependent ATPase pathway (Goodno, 1979, 1982; Wells and Bagshaw, 1984). More recently, the ternary complex of myosin S1 with ADP and BeF_3^- (M^{**}·ADP·BeF_3^-) has been shown to be analogous to M^{**}·ADP·Vi as inferred from kinetic analysis of the inhibition of myosin ATPase (Phan & Reisler, 1992) and a good analogue of the M^{**}·ADP·P_i state (Phan et al., 1993).

The heavy chain of S1 has two fast reactive thiols commonly referred to as SH1 (Cys707) and SH2 (Cys697) which can be selectively alkylated. Their reactivity has been exploited to probe the conformation of this segment of the heavy chain. The two thiols can be readily cross-linked by a variety of bifunctional sulfhydryl reagents with different spans from 14 down to 4 Å (Reisler et al., 1974), and these results suggested considerable segmental flexibility in this short segment of the heavy chain. The separation between the two thiols was estimated from FRET measurements, using extrinsic fluorescent probes covalently attached to the two sulfhydryl groups (Cheung et al., 1983). The mean intersite distance was reduced by 5−7 Å in the presence of nucleotides (Dalbey et al., 1983; Cheung et al., 1985), and the distribution of the distances between the two sites was relatively broad (Cheung et al., 1991) suggesting that the segment experienced considerable dynamic conformational fluctuation. The nucleotide-induced decrease in the mean intersite distance was time-resolved and found to occur in two kinetic steps (Garland et al., 1988). These spectroscopic results are consistent with suggestions that the ability of specific segments (including the Cys697−Cys707 segment) of the S1 heavy chain to move relative to one another is a characteristic of the energy transducing element. These movements may be necessary for the assembly and disassembly of specific sites for binding actin (Botts et al., 1989; Monet et al., 1989). An early study showed that the efficiency of energy transfer between probes attached to the single cysteine of light chain LC1 in S1 and Cys374 of actin in actosubfragment 1 was significantly increased upon addtion of ATP (Bhandari et al., 1985). Other fluorescence and chemical cross-linking studies also have provided indications of actin-modulated movements of segments of the heavy chain in the motor domain (Lin & Cheung, 1991; Bertrand et al., 1992).

The flexibility of the Cys697−Cys707 segment can be further exploited to study possible movements of the regions around the two cysteine residues of the S1 heavy chain. We have used FRET to determine distances across actoS1 from the two residues to the C-terminal Cys374 of actin and investigated the effects of the binding of ADP, orthovanadate, and beryllium fluoride on these distances. The results have yielded insights on the global conformational differences between rigor actoS1 and actoS1 species that are stable analogues of intermediate states of actomyosin in the ATPase pathway.

MATERIALS AND METHODS

Proteins. Myosin was prepared from rabbit skeletal muscle as in our previous work (Lin & Cheung, 1991). Subfragment 1 was prepared from fresh myosin using chymotryptic digestion (Weeds & Taylor, 1975), and isolated S1 was purified on a DE-52 column. The two isozymes S1(A1) and S1(A2) were pooled, dialyzed against 0.05 M ammonium acetate and 0.1 mM DTT, and lyophilized in the presence of 0.1 M sucrose. Actin was prepared from an acetone powder according to the method of Spudich and Watts (1971). An absorbance of 0.75 g^{-1} cm^{-1} at 280 nm (Wagner & Weed, 1977) and a molecular weight of 115 000 were used for the concentration of S1. An absorbance of 0.63 g^{-1} cm^{-1} at 290 nm (Houk & Ue, 1974) and a monomeric molecular weight of 42 000 were used for determination of actin concentration.

Covalent Modification of Proteins. Modification of SH1 (Cys707) with sulfhydryl reagents was carried out in the absence of nucleotide as previously described (Cheung et al., 1983, 1985). Briefly, S1 was first dialyzed against 60 mM KCl and 30 mM TES, pH 7.5, in the presence of DTT, followed by a second dialysis in which DTT was omitted. The dialyzed sample was immediately incubated on ice for 2 h with a 1.2−1.4-fold molar excess of IAEDANS initially dissolved in the same buffer. The reaction was terminated by the addition of an excess of DTT, followed by exhaustive dialysis to remove unreacted probe. This protein is designated as S1(AEDANS, SH2). When SH1 was modified with MIANS, a 1.2-fold excess of the probe initially dissolved in methanol was used. The reaction was carried out at 0 °C for 4 h in a medium containing 30 mM KCl and 50 mM HEPES, pH 8.0, followed by exhaustive dialysis. This proteins is designated as S1(MIANS, SH2). For labeling of SH2 (Cys697) of S1 with MIANS (Hiratsuka, 1992) and IAEDANS (Cheung et al., 1983), SH1 was first reacted at 4 °C for 30 min with a 2-fold molar excess of FDNB in the presence of 1 mM $MgCl_2$, 1 mM ADP, 30 mM KCl, and 50 mM HEPES, pH 8.0 (Reisler, 1982; Hiratsuka, 1992). This reversibly SH1-blocked and dinitrophenylated S1 was then reacted in the presence of 1 mM ADP and 2.5 mM $MgCl_2$ at 4 °C with a 1.3-fold molar excess of MIANS for 1 h (Hiratsuka, 1992). The corresponding reaction with IAEDANS was carried out in the presence of 5 mM ADP, 5 mM $MgCl_2$, and a 4−8-fold excess of the reagent at 4 °C for 1 h. These reactions were terminated by the addition of DTT to 10 mM, and free SH1 was regenerated from the doubly labeled S1 by incubation with 10 mM DTT at 4 °C overnight. Exhaustive dialysis against 30 mM KCl, 0.2 mM DTT, and 50 mM HEPES at pH 8.0 was used to remove the liberated dinitrophenyl group. These samples in which SH2 was modified are designated as S1(SH1, MIANS) and S1(SH1, AEDANS). The concentrations of S1 used for sulfhydryl labeling were in the range of 2−8 mg/mL.

G-actin (1−3 mg/mL) was labeled at Cys374 with a 2−4-fold molar excess of DABMI at 4 °C for 2 h, followed by the addition of an excess of DTT to stop the reactions. The labeled G-actin was dialyzed against a buffer containing 0.2 mM ATP, 0.2 mM Ca^{2+}, and 5 mM Tris at pH 8.0 and then polymerized by the addition of $MgCl_2$ to 2 mM and KCl to 50 mM at room temperature for 1 h, followed by incubation at 4 °C for several hours. The polymerized labeled actin usually was used within several days. Immediately before fluorescence measurement, the labeled F-actin was dialyzed against 10 mM KCl, 1 mM $MgCl_2$, and 10 mM Tris, pH 8.0, to remove free nucleotide.

The degrees of labeling of S1 and actin by various probes were calculated using the following molar absorption coefficients (1 cm path): IAEDANS, 6100 at 337 nm; MIANS, 17 000 at 327 nm; DABMI, 24 800 at 460 nm; and FDNB, 11 000 at 339 nm. With FDNB, IAEDANS, and DABMI, the degrees of labeling of SH1 in S1 were in the range of 0.96−0.99, while the labeling stoichiometry of SH2 was about 0.9 with both IAEDANS and MIANS. The degree of labeling of actin by DABMI was in the range of 0.96−0.99.

ATPase Assays. Labeled S1 was routinely assayed for both Ca^{2+}-ATPase and K^+/EDTA-ATPase activities by determination of phosphate release (Fiske & SubbaRow, 1925). The assays were carried out at room temperature in 0.6 M KCl, 0.9 mM ATP, and 50 mM Tris at pH 8.0, and either 9 mM $CaCl_2$ or 10 mM EDTA. The typical activity of unmodified S1 was in the range of 1.4−1.6 μmol of P_i/μmol of S1/s for the Ca^{2+}-ATPase and 8.1−8.6 μmol of P_i/μmol of S1/s for the K^+/EDTA-ATPase.

Fluorescence Measurements. Steady-state fluorescence measurements were carried out in an SLM 8000C spectrofluorometer at 20 °C unless indicated otherwise. All measurements were made with protein samples in a medium containing 60 mM KCl, 2 mM $MgCl_2$, 0.1 mM DTT, and 50 mM HEPES at pH 8.0. The concentration of S1 was in the range of 1−3 μM. When present, ADP was 2 mM, Vi was 0.4 mM, and BeF was 0.1−0.2 mM. All emission spectra were corrected for variation of the detector system as a function of wavelengths. The excitation wavelength was 330 nm for proteins labeled with IAEDANS and 340 nm for MIANS-labeled S1. Quantum yields were determined by the comparative method (Parker & Reese, 1960), using quinine bisulfate in 0.1 N H_2SO_4 (quantum yield 0.70) as the standard (Scott et al., 1970). Polarization measurements were made using the T-format of the spectrofluorometer. Fluorescence intensity decay was determined in a PRA-2000 photon-counting pulsed nanosecond spectrometer as previously described (Aguirre et al., 1989). The anisotropy decay function was obtained from the fluorescence intensities polarized in the vertical and horizontal directions, $F_{||}(t)$ and $F_{\perp}(t)$, respectively,

$$A(t) = \frac{F_{||}(t) - F_{\perp}(t)}{F_{||}(t) + 2F_{\perp}(t)} \tag{1}$$

and deconvoluted by a nonlinear least-squares algorithm (Grinvald & Steinberg, 1974). The $A(t)$ function was assumed to follow either a monoexponential or a biexponential decay law:

$$A(t) = r_o \sum_{i=1}^{2} g_i \exp(-t/\theta_i) \tag{2}$$

where θ_i are the rotational correlation times with fractional amplitudes g_i, and r_o is the limiting anisotropy at zero time.

Determination of Energy Transfer. The efficiency of fluorescence resonance energy transfer (E) was calculated from steady-state emission data using the following expression (Cheung, 1991):

$$E = 1 - \frac{F_{da} - F_d(1 - f_a)}{F_d f_a} \tag{3}$$

where F_d is the fluorescence intensity of the donor determined at a given wavelength in the absence of an acceptor, F_{da} is the intensity of the donor determined in the presence of an acceptor, and f_a is the fraction of acceptor sites occupied by the acceptor. Alternatively, the quantum yield (integrated emission spectrum) could be used instead of the intensity at a single wavelength. The two protocols yielded very comparable results within 2−3% in several preliminary experiments. In subsequent experiments, intensity data determined from a single wavelength were used to calculate E. The separation (R) between donor and acceptor sites was calculated from

$$E = \frac{R_o^6}{R_o^6 + R^6} \tag{4}$$

In this equation R_o is the Förster critical distance at which the transfer efficiency is 0.5 and is given by

$$R_o^6 = (8.79 \times 10^{-5}) n^{-4} Q \kappa^2 J \, (\text{Å})^6 \tag{5}$$

where n is the refractive index of the solution (taken as 1.4), Q is the donor quantum yield, κ^2 is the orientation factor, and J is the overlap integral:

$$J = \frac{\int F_d(\lambda) \epsilon_a(\lambda) \lambda^4 \, d\lambda}{\int F_d(\lambda) \, d\lambda} \tag{6}$$

$F_d(\lambda)$ is the fluorescence intensity of the donor at wavelength λ, and $\epsilon_a(\lambda)$ is the molar absorption of the acceptor at λ. The overlap integral was evaluated by numerical integration. In the systems reported here, the donor probe was attached to one protein and the acceptor probe to another protein. The distance which was determined was an intermolecular distance of the binary protein complex. To ensure that appropriate spectroscopic properties of probes attached to the proteins were used in the calculation of distances, the quantum yield of a donor probe attached to S1 was determined in the presence of a large excess of the other unlabeled protein (actin), and the absorption spectrum of an acceptor attached to actin was similarly measured. Of the probes used, IAEDANS and MIANS served as energy donor, whereas the nonfluorescent probe DABMI served as energy acceptor. The reported distances are averages determined from several preparations of proteins.

Electrophoresis. Labeled S1 was digested with trypsin and hydroxylamine as previously described (Cheung et al., 1983). The digested fragments were separated on either 12% (tryptic digest) or 15% (hydroxylamine digest) sodium dodecyl sulfate−polyacrylamide gels. Fluorescent fragments were located on unstained gels under UV illumination (Cheung et al., 1983).

Reagents and Chemicals. ADP, ATP, and chymotrypsin were obtained from Sigma Chemical Co. (St. Louis, MO) and used without further purification. A stock solution of sodium vanadate was prepared from V_2O_5 obtained from Aldrich Chemical Co. (Milwaukee, WI) as described by Goodno (1982). BeF was prepared from standard solutions of $BeCl_2$ (0.1 mM) and NaF (5 mM) obtained from Sigma Chemical Co., using a 3−4-fold stoichiometric excess of fluoride. All other chemicals were of reagent grade.

RESULTS

Characterization of Labeled Proteins. A total of five labeled proteins were prepared with three different sulfhydryl

reagents: four labeled S1 and one labeled actin. One set of three labeled proteins were used to map the distance between actin Cys374 and SH1 of S1 in rigor A•S1 and A•S1 in the presence of ligands. This distance was determined with two binary A•S1 complexes bearing different donor−acceptor pairs between the two sites: A(DABM)•S1(MIANS, SH2) and A(DABM)•S1(AEDANS, SH2). The second set of labeled proteins was used to determine the distance between actin Cys374 and SH2 of S1 in A•S1, using MIANS and AEDANS attached to SH2 as energy donors and DABM attached to actin as energy acceptor: A(DABM)•S1(SH1, MIANS) and A(DABM)•S1(SH1, AEDANS).

The labeling of SH1 with IAEDANS enhanced the Ca^{2+}-ATPase activity by a factor of 3−4 and inhibited the K^+/EDTA-ATPase activity by at least 90%. These results are in agreement with previous reports on the effect of SH1 modification by this and some other reagents (Cheung et al., 1983). The changes in these two types of ATPase activity are known to parallel the extent of SH1 labeling by IAEDANS, and the ATPase activities indicated that the dominant site which was labeled was SH1.

When SH1 was modified with MIANS, the Ca^{2+}-ATPase activity was enhanced by a factor of 1.6 and the K^+/EDTA-ATPase activity was reduced by 55%. These changes were in the same directions as those observed with S1 modified at the same site with IAEDANS, but the changes were smaller. The smaller changes were not due to undermodification of SH1 because the degree of labeling was over 95%. Subsequent treatment of the MIANS-labeled sample with NEM did not change the ATPase activities. The MIANS-labeled S1 was tryptic digested, followed by treatment with hydroxylamine (Cheung et al., 1983), and the digests were run on sodium dodecyl sulfate−polyacrylamide gels. Upon UV illumination, the fluorescence of the MIANS moiety was found only on the 20-kDa band from the tryptic digest and on the 13-kDa band from the hydroxylamine digest. No fluorescence was observed in the small fragment (7 kDa) from the hydroxylamine digest. These results (not shown) indicated that MIANS modified SH1 (13-kDa band) and not SH2 (7 kDa) or other sites.

The labeling of SH2 with MIANS or IAEDANS required prior blocking of SH1 by FDNB and subsequent regeneration of free SH1 by thiolysis. The degrees of labeling of SH2 by these probes were determined from their absorbance. The absorption peaks of FDNB, MIANS, and AEDANS are in the 325−340 nm range. It was necessary to establish that the attached FDNB probe was fully released by thiolysis so that SH1 was completely regenerated and that there was no spectral interference from residual FDNB in the determination of labeling stoichiometry by the fluorescent probes at SH2. Control experiments showed that FDNB was fully released from S1 singly modified by FDNB after incubation with 10 mM DTT overnight, as evidenced from the loss of the FDNB absorption band. The Ca^{2+}-ATPase activity of FDNB-modified S1 was enhanced by a factor of 3−4, and the K^+/EDTA-ATPase activity was better than 90% inhibited. After thiolysis, the Ca^{2+}-ATPase activity returned to that of unmodified S1 prior to modification (within experimental error) and the lost K^+/EDTA-ATPase activity was restored. These ATPase activity results were supported by absorption results indicating the residual amount of attached FDNB to be negligible after thiolysis.

S1 doubly labeled with FDNB and MIANS at SH1 and SH2, respectively, was greatly inhibited in both the Ca^{2+}-ATPase and K^+/EDTA-ATPase activities. These results indicated that the dominant site modified by MIANS was SH2. When compared with native unmodified S1, the specific Ca^{2+}-ATPase activity of S1 modified at SH2 with MIANS (after free SH1 was regenerated) was unchanged (e.g., 1.61 μmol of P_i/μmol of S1/s vs 1.59 μmol of P_i/μmol of S1/s with one preparation), but the K^+/EDTA-ATPase activity was reduced by 58%. The fluorescence of the MIANS moiety was localized on the small 7-kDa fragment and not on the 13-kDa fragment generated by digestion of labeled S1 with trypsin, followed by hydroxylamine. Thus, the dominant site labeled by MIANS in the SH1-regenerated sample was SH2.

The Ca^{2+}-ATPase activity of S1 singly labeled at SH2 with IAEDANS was about 85% of unmodified S1, and the K^+/EDTA-ATPase activity was about 50% inhibited. The dominant site which was labeled with IAEDANS after SH1 was blocked was previously shown to be SH2 on the basis of changes of ATPase activities and localization of the fluorescence of the AEDANS moiety on the 7-kDa hydroxylamine fragment (Cheung et al., 1983).

Equilibrium Concentrations in Mixtures of Actin, S1, and Nucleotide. The determination of an intersite distance across the binary rigor complex A•S1 from energy transfer data was straightforward from eqs 3−5. The quantum yield of the donor and F_d were readily determined from donor-labeled S1 in the presence of a large excess of unlabeled actin, and F_{da} was measured with a sample of A•S1 which was prepared from donor-labeled S1 with a large excess of acceptor-labeled actin. The concentration of uncomplexed donor-labeled S1 in these samples was negligible, and all donor-labeled S1 molecules in the A•S1 sample containing acceptor-labeled actin participated in energy transfer. The fluorescence parameters determined from these samples reflected accurately the properties of the donor in the binary complex. In the presence of ADP, however, a set of multiple equilibria existed among the four species S1, S1•ADP, A•S1, and A•S1•ADP. Donor-labeled S1 was partitioned into all four species, and the measured values of Q, F_d, and F_{da} were composite values which contained contributions from all four species. For the determination of energy transfer across actoS1 in the ternary complex A•S1•ADP, the observed fluorescence parameters must be corrected for contributions of fluorescence signal from free labeled S1 and from the two binary complexes S1•ADP and A•S1. At equilibrium the concentrations of the four species are governed by

Scheme 1

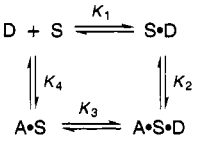

where D is ADP, S is S1, and A is actin. The equilibrium concentrations for a given set of initial concentrations of actin, S1, and ADP can be readily calculated from the four equilibrium constants, using an iterative procedure. A set of typical results is given in Table 1. Results similar to those shown in Table 1 allowed calculations of Q, F_d, and F_{da} for the ternary complex A•S1•ADP from the observed fluores-

Table 1: Equilibrium Concentrations of Various Species in Mixture of Actin, Myosin S1, and ADP in the Absence and Presence of Vanadate[a]

initial concentration (μM)		equilibrium concentrations (μM)	
		scheme 1	scheme 2
[actin]: 10	$[S1]_{free}$	0.0002 (0.01%)	0
[S1]: 2	[A·S1]	0.077 (3.9%)	0.0005 (0.025%)
[ADP]: 2000	[S1·ADP]	0.50 (24.9%)	0.003 (0.15%)
	[A·S1·ADP]	1.42 (71.2%)	0.009 (0.45%)
[Vi]: 400	[S1·ADP·Vi]		1.36 (67.8%)
	[A·S1·ADP·Vi]		0.63 (31.5%)

[a] In the absence of vanadate, the equilibrium concentrations were calculated from Scheme 1. In the presence of vanadate, the concentrations were calculated from Scheme 2. The species listed in the table are those which contain S1, and the species containing no S1 are not given. The following equilibrium constants were used in the calculations: $K_1 = 1.4 \times 10^6\ M^{-1}$ (Aguirre et al., 1986), $K_2 = 4 \times 10^5\ M^{-1}$ (Geeves, 1989), $K_3 = 6 \times 10^3$ (Geeves, 1989), $K_4 = 1.5 \times 10^7\ M^{-1}$ (Lin et al., 1993), $K_5 = 1.2 \times 10^6\ M^{-1}$, $K_6 = 5 \times 10^4\ M^{-1}$, and $K_7 = 2 \times 10^3\ M^{-1}$. The values of K_1–K_4 were determined at 20 °C in 60 mM KCl, pH 7.0–7.5. The other three constants were determined at 15 °C in 1 mM KCl, pH 7.0 (Smith & Eisenberg, 1990).

cence. Under the initial concentrations shown, $[S1]_{free}$ was negligible and the observed Q, F_d, and F_{da} contained no contribution from uncomplexed labeled S1. The concentrations of A·S1·ADP and S1·ADP were 71% and 25% of the total [S1], respectively. The donor in S1·ADP contributed significantly to the three observed fluorescence parameters. While the concentration of the binary complex A·S1 was less than 4% of the initial [S1], the fluorescence contribution from this complex containing both donor and acceptor reflected energy transfer which occurred in the binary complex. The relative concentrations of A·S1 and S1·ADP could be decreased by increasing the initial actin concentration or total protein concentrations. In the experiments reported here, the initial concentration of donor-labeled S1 was kept below 3 μM in order to minimize inner filter effects in fluorescence measurements. It was necessary to keep total actin concentration at or below 10 μM to avoid excessive scattering and viscosity problems arising from high concentrations of actin filaments. The contribution of donor fluorescence from the equilibrium concentration of S1·ADP was determined with an S1·ADP sample prepared from donor-labeled S1 at a concentration equal to the calculated equilibrium concentration of S1·ADP with a large excess of ADP. The contribution of donor fluorescence from A·S1 was similarly determined. The observed fluorescence was then corrected for the contributions from these two complexes.

In the presence of a phosphate analogue (L) at saturating ADP concentration, it was necessary to include three additional steps (Scheme 2) for formation of the ternary complex S1·ADP·L (K_5) and the complex A·S1·ADP·L from S1·ADP·L (K_6) and A·S1·ADP (K_7):

Scheme 2

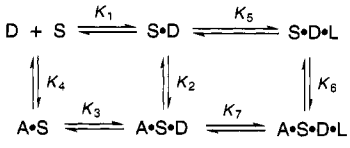

The equilibrium concentrations of the various species can be estimated from a set of initial concentrations of A, S, and L. The additional constants (K_5, K_6, K_7) for L = Vi were taken from Smith and Eisenberg (1990) which were determined with alkylated S1 at a low ionic strength, and for L = BeF they were taken from Phan et al. (1993) determined at 40 mM KCl. A set of calculated equilibrium concentrations from Scheme 2 with vanadate as the ligand are also given in Table 1 for comparison with the concentrations in the absence of vanadate. The dominant equilibrium species in Scheme 2 are A·S1·ADP·Vi and S1·ADP·Vi. The concentrations of the other S1-containing species are negligibly small (less than 1% total). Thus, for the determination of energy transfer across actoS1 in the A·S1·ADP·Vi complex, only the contribution of the donor fluorescence in S1·ADP·Vi needed to be determined and subtracted from the observed fluorescence. With BeF the dominant species is S1·ADP·BeF (>80%) with A·S1·ADP·BeF being less than 10%. Because of the unfavorable equilibrium concentration of the A·S1 complex containing bound ADP and BeF, it was difficult to correct for the concentrations of S1 species containing donor and ligands, and no energy transfer was determined for A·S1·ADP·BeF.

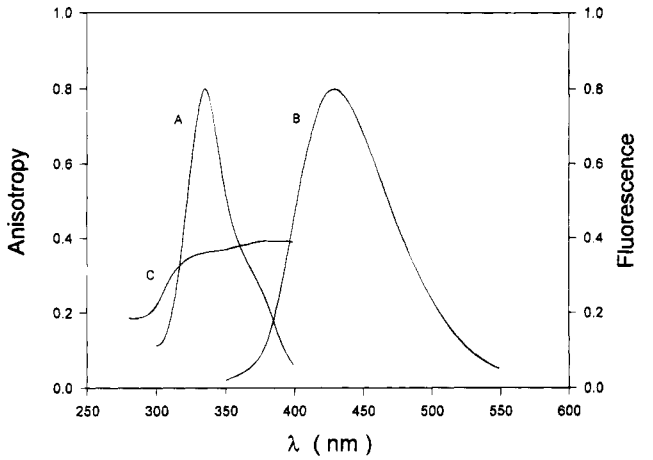

FIGURE 1: Fluorescence spectra of the adduct of MIANS and β-mercaptoethanol in glycerol at −4 °C. (A) Excitation spectrum recorded with λ_{em} at 450 nm. (B) Emission spectrum with excitation wavelength at 340 nm. (C) Anisotropy spectrum as a function of excitation wavelength, with λ_{em} at 450 nm.

Spectral Properties of MIANS-Labeled S1. MIANS was reacted with β-mercaptoethanol, and the adduct was used to study the fluorescence properties of the MIANS moiety. Figure 1 shows the fluorescence excitation and emission spectra and the anisotropy as a function of excitation wavelength of the adduct in glycerol at −4 °C. The emission peak was at 436 nm as compared with a value of 453 nm determined in aqueous solution, at pH 7 and 20 °C (data not shown). The anisotropy values across the long-wavelength absorption band approached 0.4 at the red edge of the absorption band.

The effects of ADP and ADP plus Vi on the emission spectrum of MIANS attached to SH2, S1(SH1, MIANS), are shown in Figure 2. The spectral parameters are listed in Table 2. The emission maximum of the probe attached SH2 was blue-shifted by 29 nm to 424 nm when compared to that in an aqueous medium. ADP and ADP plus Vi decreased the quantum yield of S1(SH1, MIANS) by 31 and 50%, respectively. The decrease was accompanied by a 6-nm red-shift. The decrease of quantum yield induced by ADP plus BeF was 49%, and the quenched spectrum was very similar to curve 3, but with a 2-nm red-shift (λ_{em} =

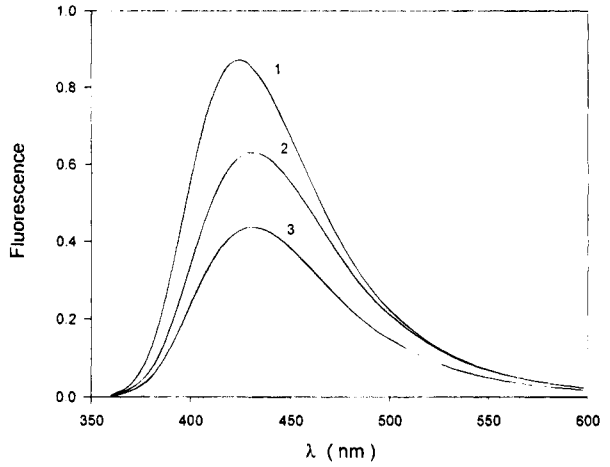

FIGURE 2: Fluorescence emission spectrum of S1 labeled at SH2 with MIANS: S1(SH1, MIANS). In this sample, SH1 was first labeled with FDNB prior to labeling of SH2, followed by regeneration of free SH1 using DTT. Curve 1, labeled S1 alone (1 μM); curve 2, labeled S1 (1 μM) + MgADP (2 mM); and curve 3, labeled S1 (1 μM) + MgADP (2 mM) + Vi (0.4 mM). Other conditions are given in the text.

Table 2: Fluorescence Properties of Myosin S1 Labeled at SH1 and SH2 with MIANS[a]

protein/labeled site	ligand	λ_{em} nm	rel Q
S1/SH2		424	1.0
	ADP	430	0.69
	ADP, Vi	430	0.50
	ADP, BeF	432	0.49
	ATP	434	0.61
	ADP (after ATP depletion)	429	0.71
A·S1/SH2		426	0.90
	ADP	422	1.05
	ADP, Vi	416	0.78
	ATP	434	0.67
	ADP (after ATP depletion)	422	0.78
S1/SH1		428	1.0
	ADP	430	0.84
	ADP, Vi	434	0.51
	ADP, BeF	432	0.83
	ATP	432	0.87
	ADP (after ATP depletion)	432	0.89
A·S1/SH1		430	1.0
	ADP	428	1.07
	ADP, Vi	428	0.80
	ATP	432	0.87
	ADP (after ATP depletion)	430	0.89

[a] For S1/SH2 and A·S1/SH2, rel Q is the relative quantum yield normalized to the quantum yield of S1/SH2 determined in the absence of ligands. Rel Q for S1/SH1 and A·S1/SH1 was normalized to the quantum yield of S1/SH1 in the absence of ligands. The parameters in the presence of ATP (100 μM) were determined from spectra obtained within 10−25 s after addition of ATP. The spectra of those samples were recorded again after depletion of ATP, approximately 1000 s later. [S1] = 2 μM, [A] = 10 μM, and other conditions are given in the text.

332 nm, spectrum not shown). The presence of an inorganic phosphate analogue resulted in a substantially lower quantum yield of the attached MIANS, and this decrease was due to formation of the ternary complex S1·ADP·Vi or S1·ADP·BeF. MIANS attached to SH2 experienced a substantial fluorescence quenching and sensed a more polar environment when the active site pocket was occupied by ADP or ADP plus a phosphate analogue.

When ATP (0.1 mM) was added to S1(SH1, MIANS) (1.5−5 μM), the steady-state emission intensity immediately decreased by about 40%, which remained constant for a period of time and then began to increase slowly and reached a second constant level as previously reported (Hiratsuka, 1992). As has been shown, the first region of constant fluorescence intensity was due to ATP hydrolysis in the steady state, and the second region of constant intensity reflected depletion of ATP. The emission spectra obtained within 25 s of ATP addition and at the early stage of the steady state showed a 10-nm red-shift (emission peak at 434 nm) with a 40% reduction in quantum yield (Table 2). The spectrum obtained after ATP depletion showed an emission peak at 429 nm with a relative quantum yield of 0.71 when compared to S1(SH1, MIANS) prior to the addition of ATP. These spectral properties were characteristic of the complex S1(SH1, MIANS)·ADP in which bound ADP was generated at the active site from ATP hydrolysis and were very similar to the properties observed by adding ADP to S1(SH1, MIANS). The emission peak of MIANS during the steady-state hydrolysis suggested a much more polar environment than in the absence of any bound ligand at the active site. At the end of hydrolysis, the spectrum blue-shifted back to about the same position as that observed by adding ADP.

Table 3: Fluorescence Properties of Myosin S1 Labeled at SH1 and SH2 with IAEDANS[a]

protein/labeled site	ligand	λ_{em} nm	rel Q
S1/SH2		486	1.0
	ADP	486	0.92
	ADP, Vi	488	0.71
A·S1/SH2		484	1.0
	ADP	486	0.96
	ADP, Vi	484	0.81
S1/SH1		488	1.0
	ADP	488	1.06
	ADP, Vi	490	0.82
A·S1/SH1		486	1.14
	ADP,	487	1.06
	ADP, Vi	484	0.84

[a] For S1/SH2 and A·S1/SH2, rel Q is the relative quantum yield normalized to the quantum yield of uncomplexed S1/SH2 in the absence of ligands. For S1/SH1 and A·S1/SH1, rel Q was normalized to the quantum yield of uncomplexed S1/SH1 in the absence of ligands. See Table 2 and text for other conditions.

The spectral properties of MIANS covalently attached to SH1 in S1(MIANS, SH2) are given in Table 2. The emission maximum was 25 nm blue-shifted relative to an aqueous environment, but it was 4 nm longer than that observed with the probe attached to SH2. Bound ligands induced small red spectral shifts (2−6 nm), as were detected with S1(SH1, MIANS). The ligands also decreased the quantum yield to varying extents. The addition of ATP immediately reduced the relative quantum yield to 0.84 with a 4-nm red-shift, and at the end of the hydrolysis the relative quantum yield increased only slightly to 0.89, about the same as that determined by the addition of ADP to S1(MIANS, SH2). Although the increase in quantum yield at the end of hydrolysis was very small, the increase was reproducibly demonstrated by monitoring the emission intensity at a single wavelength as a function of time (results not shown).

S1 Labeled with IAEDANS. IAEDANS was used as a second probe to examine the immediate environments of SH1 and SH2. The fluorescence spectral properties of this probe attached to the two sites in isolated S1 and in the respective actoS1 complexes are given in Table 3. With uncomplexed

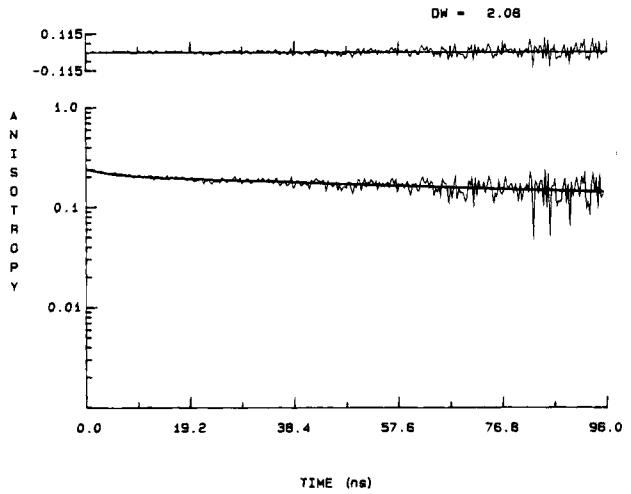

FIGURE 3: Representative plot for the fluorescence anisotropy decay of S1 labeled with IAEDANS at SH2: S1(SH1, IAEDANS). The data were collected at 20 °C and fitted to a biexponential function, yielding two rotational correlation times: $\theta_1 = 3.7$ ns, $\theta_2 = 248$ ns; $r_0 = 0.274$. $\chi_R^2 = 1.13$, D−W (Durbin−Watson number) = 2.08. The panel across the top of the figure is the residual plot of the best fitted data. Two intensity decay times were recovered from the anisotropy decay data, $\tau_1 = 7.7$ ns and $\tau_2 = 20.4$ ns, and these values were in good agreement with the values obtained from a direct analysis of intensity decay data. The excitation light was isolated with a 350-nm three-cavity interference filter, and the emission was isolated with a Corning 3-73 cut-off filter. [S1] = 30 μM, and other conditions are given in the text.

S1, the wavelengths of maximum fluorescence intensity were blue-shifted by 18 and 16 nm for SH2 and SH1, respectively, from that observed in an aqueous environment (504 nm). Small red spectral shifts and small decreases in quantum yield were observed in the presence of ADP and ADP plus Vi, but these changes were not sufficient to establish a clear pattern. The Ca^{2+}-ATPase activity of S1 singly modified with IAEDANS at SH1 was considerably larger than S1 modified with MIANS. The larger activity made it difficult to acquire the emission spectrum during the steady-state hydrolysis of ATP.

Anisotropy Decay of Labeled S1. The anisotropy decay of S1 separately labeled at SH1 and SH2 with the two donor probes was measured to determine the limiting anisotropy values. A representative anisotropy decay plot is shown in Figure 3 for S1 labeled at SH2 with IAEDANS. The decay was fitted to the sum of two exponential terms with two rotational correlation times. The long correlation time was typical of that for the overall motion of S1, and the short correlation time reflected limited motion of the attached probe. This limited probe motion was observed with both AEDANS and MIANS linked to either SH1 or SH2. The limiting anisotropy values for the two attached probes are listed in Table 4.

Spectral Properties of MIANS-Labeled S1 Complexed with Actin. Figure 4 (curves 1−3) shows the emission spectrum of actoS1 in which S1 was labeled with MIANS at SH2 and the effects of ADP and ADP plus Vi on the emission properties of the complex. The spectral parameters for these actoS1 complexes are given in Table 2. The addition of actin resulted in a 10% decrease in quantum yield and a small red spectral shift, suggesting rigor formation of A·S1 being accompanied by an exposure of MIANS attached to SH2. When ADP was added to A·S1(SH1, MIANS), the observed emission spectrum reflected the presence of not only the

Table 4: Anisotropy and Axial Depolarization of Probes Attached to S1[a]

probe	site	r_0	$\langle d^x \rangle$	κ^2(min)	κ^2(max)
MIANS	SH2	0.301	0.900	0.050	3.80
	SH1	0.306	0.917	0.040	3.85
IAEDANS	SH2	0.209	0.988	0.015	3.95
	SH1	0.205	0.979	0.020	3.90

[a] The axial depolarization factor was calculated from $\langle d^x \rangle = (r_0/r_f)^{1/2}$, where r_0 is the zero-time anisotropy and r_f is the fundamental anisotropy experimentally determined at a low temperature and in a high-viscosity medium. r_f was 0.364 for MIANS and 0.214 for IAEDANS. κ^2(min) and κ^2(max) are the minimum and maximum values of the orientation factor and were calculated from $\langle d^x \rangle$.

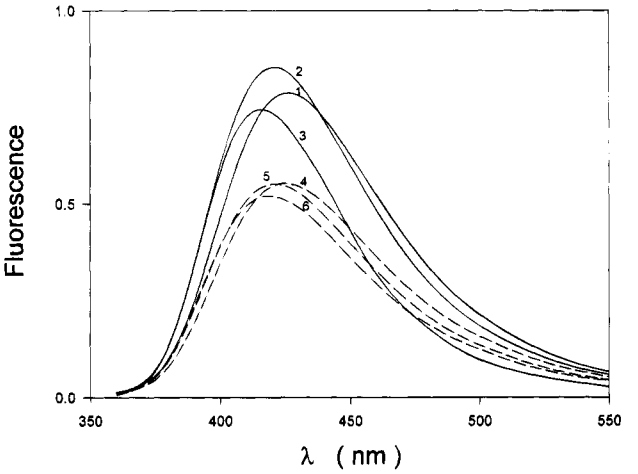

FIGURE 4: Fluorescence resonance energy transfer between actin Cys374 and SH2 of myosin S1 in the complex actoS1, using MIANS and DABMI as energy donor and acceptor, respectively. Actin was either unlabeled or labeled at Cys374 with acceptor, and SH2 was labeled with donor. Curves 1−3 are the emission spectra of donor MIANS in the complex formed with unlabeled actin for the three states: rigor complex A·S1 (curve 1), A·S1·ADP (curve 2), and A·S1·ADP·Vi (curve 3). Curves 4−6 are the emission spectra of donor MIANS in actoS1 formed with acceptor-labeled actin for the three states: rigor A·S1 (curve 4), A·S1·ADP (curve 5), and A·S1·ADP·Vi (curve 6). The spectra for the complexes containing ADP and Vi have been corrected for contributions from other donor-labeled S1 species as described in the text. Spectra equivalent to curves 1 and 4, curves 2 and 5, and curves 3 and 6 were used to determine the transfer efficiency for rigor A·S1, A·S1·ADP, and A·S1·ADP·Vi. [S1] = 2 μM, [actin] = 10 μM, [$MgCl_2$] = 2 mM, [Vi] = 0.4 mM, and other conditions are given in the text.

ternary complex A·S1·ADP but also other species containing MIANS (S1·ADP, A·S1, and uncomplexed S1). To obtain the emission spectrum of the ternary complex A·S1·ADP, the contributions from these species to the observed spectrum were separately determined, and the observed spectrum was corrected for these contributions (curve 2). A similar procedure was used to obtain the spectrum for A·S1·ADP·Vi (curve 3). The spectral parameters for these actoS1 species are also listed in Table 2. The spectrum of the ternary complex A·S1·ADP was blue-shifted by 4 nm with a small increase in quantum yield when compared with the binary complex A·S1. The formation of the complex A·S1·ADP·Vi resulted in a further blue-shift of 6 nm and a decrease in quantum yield. These spectral shifts induced by ADP and ADP plus Vi were in the opposite direction of those observed in the absence of actin, while the decreases in quantum yield were smaller. Upon addition of ATP to A·S1(SH1, MIANS), spectral changes similar to those detected with uncomplexed S1(SH1, MIANS) were also observed. During the early

stage of ATP hydrolysis, the emission maximum was 434 nm, identical to the value observed with uncomplexed S1.

The effect of actin on the spectral maximum of S1 labeled at SH1 with MIANS, S1(MIANS, SH2), was a small red-shift (Table 2), similar to the effect of actin on S1 labeled at SH2. The effects of nucleotides and phosphate analogues on the wavelength of maximal intensity and quantum yield of MIANS attached to SH1 were also similar to those of the probe attached to SH2. MIANS sensed a more polar environment of SH1 during the steady-state hydrolysis of ATP, as it did on the environment of SH2. The effects of nucleotides on the fluorescence properties of MIANS at SH1 were not as pronounced as those observed with MIANS attached to SH2.

Energy Transfer across ActoS1. DABMI has a broad absorption band with a maximum near 460 nm which overlaps the fluorescence emission spectrum of IAEDANS (Miki et al., 1986). A similar sepctral overalp is observed between DABMI and MIANS (data not shown). These spectral overlaps provide the basis of resonance energy transfer between the two fluorophores and DABMI. A typical set of energy transfer data between MIANS (donor) attached to SH2 of S1 and DABM (acceptor) attached to actin Cys374 in A·S1 are shown in Figure 4 (curves 4−6). Curve 1 is the emission spectrum of actoS1 formed between donor-labeled S1 and unlabeled actin. Curve 4 is the corresponding spectrum obtained with actin labeled at Cys374 with the acceptor DABMI under the same protein concentrations. The large decrease in the area of the spectrum was indicative of transfer of resonance energy from MIANS in S1 to DABM in actin within the binary complex. Control experiments with actin labeled at Cys374 with NEM showed a negligible decrease in the area of the emission spectrum obtained from the complex. Thus, the large intensity decrease observed with DABM-labeled actin resulted from transfer of resonance energy between the two probes. These two spectra contained information needed to calculate the transfer efficiency between the two sites across rigor actoS1. Curve 2 is the corrected spectrum of the ternary complex A·S1·ADP obtained with donor-labeled S1 and unlabeled actin, and curve 5 is the corresponding spectrum obtained with donor-labeled S1 and acceptor-labeled actin. Curves 3 and 6 are the spectra for A·S1·ADP·Vi obtained with unlabeled actin and acceptor-labeled actin, respectively. The transfer efficiency between the two sites was calculated from these spectra for the complexes A·S1·ADP and A·S1·ADP·Vi.

Figure 5 shows the emission spectra of actoS1 in which SH1 of S1 was labeled with MIANS and actin Cys374 was either unlabeled or labeled with DABMI for rigor A·S1 and its complexes with ADP and ADP + Vi. These spectra show large decreases in intensity when actin was labeled with the acceptor DABMI, and spectra similar to these were used to determine the transfer efficiency between actin Cys374 and SH1 in different actoS1 states.

Three sets of intersite distances were calculated, for each biochemical state, from the observed transfer efficiency between each pair of sites. The first set was based on the assumption of random and rapid orientations of the transition dipoles ($\kappa^2 = {}^2/_3$) of both donor and acceptor. The other two sets were calculated from the estimated upper and lower bounds of the orientation factor as in our previous work (Wang & Cheung, 1986) according to Dale et al. (1979).

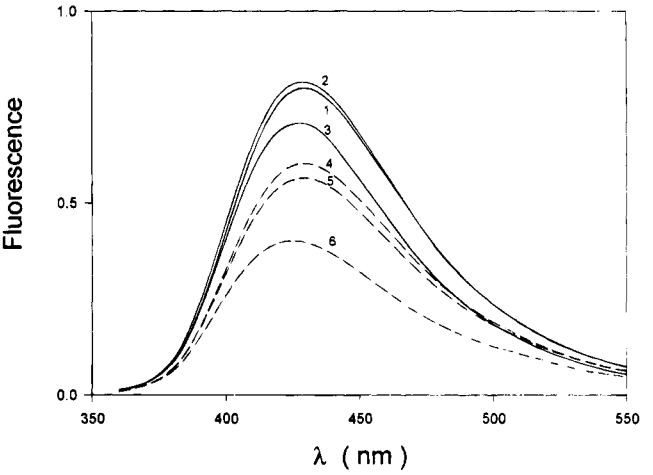

FIGURE 5: Fluorescence resonance energy transfer between actin Cys374 and SH1 of myosin S1 in the complex actoS1, with MIANS attached to SH1 as energy donor and DABMI attached to Cys374 as energy acceptor. Curves 1, 2, and 3 are the emission spectra of donor MIANS in actoS1 obtained with unlabeled actin for rigor A·S1 (curve 1), A·S1·ADP (curve 2), and A·S1·ADP·Vi (curve 3). Curves 4−6 are the corresponding curves obtained with acceptor-labeled actin for rigor A·S1 (curve 4), A·S1·ADP (curve 5), and A·S1·ADP·Vi (curve 6). Conditions are the same as given for Figure 5.

The limiting anisotropy values obtained from anisotropy decay measurements were used in the calculation of the depolarization factors. The calculated distances between actin Cys374 and SH2 of S1 for the three complexes A·S1, A·S1·ADP, and A·S1·ADP·Vi are given in Table 5, and the distances between actin Cys374 and SH1 for the same complexes are given in Table 6. The precision of the energy transfer experiment is dependent upon the random errors in the experimental values of E, Q, and J and the uncertainty of the binding constants used to calculate the concentrations of several S1-containing species. The errors in $R({}^2/_3)$ can be estimated using the standard procedures for propagation of random errors and, for the experiments reported here, were found to be in the range of 1.2−2.3 Å. Ligand-induced changes in $R({}^2/_3)$ larger than 2.5 Å may be considered beyond random experimental uncertainty.

The distance between actin Cys374 and SH1 in rigor A·S1 (A·S1) is sensitive to ligand binding regardless of whether the probe was MIANS or AEDANS. The distance $R({}^2/_3)$ was reduced by 7−8 Å in the presence of ADP + Vi, although ADP alone did not induce a significant decrease. The values of R(min) and R(max) also showed similar ligand-induced changes. The distance between Cys374 and SH2, however, was little or not affected by the either ADP or ADP plus Vi.

DISCUSSION

We have used two fluorescent probes to study the immediate environments of the two fast reactive thiols, SH1 and SH2, of the heavy chain of myosin subfragment 1. The two probes MIANS and IAEDANS have slightly different structures and different environmental sensitivities. When used together to probe the same two sites, they can provide a better description of the local environments, and the results allow us to compare the properties of the two sites in a more direct manner since each of the fluorophores is used to probe both sites. These probes are also used as donors of

Table 5: Energy Transfer between Actin Cys374 and Myosin SH2 (Cys697) in the ActoS1 Complex[a]

donor	species	E	Q	$J \times 10^{-15}$ (cm^{-1} M^{-1} nm^4)	$R(^2/_3)$ (Å)	R(min) (Å)	R(max) (Å)
MIANS	A·S1	0.298	0.273	0.774	44.3	28.8	59.3
	A·S1·ADP	0.352	0.303	0.754	43.1	28.0	57.6
	A·S1·ADP·Vi	0.273	0.237	0.724	43.7	28.4	58.4
IAEDANS	A·S1	0.317	0.479	0.722	47.4	28.3	63.6
	A·S1·ADP	0.331	0.463	0.715	46.6	27.8	62.5
	A·S1·ADP·Vi	0.286	0.387	0.724	46.9	28.0	63.0

[a] Actin Cys374 was labeled with energy acceptor DABMI, and myosin SH2 was labeled with either MIANS or AEDANS as energy donor. All measurements were carried out at 20 °C in 60 mM KCl, 2 mM $MgCl_2$, 0.1 mM DTT, and 50 mM HEPES at pH 8.0. [ADP] = 2 mM, [Vi] = 0.4 mM, and see text for the ranges of protein concentrations. $R(^2/_3)$ is the donor−acceptor distance calculated from energy transfer data assuming the orientation factor $\kappa_2 = {}^2/_3$. R(min) and R(max) are the minimum and maximum distances, respectively, calculated from the estimated lower and upper bounds of κ^2. The uncertainty in the calculated $R(^2/_3)$ due to random errors in energy transfer measurements is estimated at ±2.5 Å (see text).

Table 6: Energy Transfer between Actin Cys374 and Myosin SH1 (Cys707) in the ActoS1 Complex[a]

donor	species	E	Q	$J \times 10^{-15}$ (cm^{-1} M^{-1} nm^4)	$R(^2/_3)$ (Å)	R(min) (Å)	R(max) (Å)
MIANS	A·S1	0.245	0.244	0.784	45.6	29.6	60.9
	A·S1·ADP	0.305	0.254	0.782	43.6	28.3	56.2
	A·S1·ADP·Vi	0.438	0.222	0.777	38.7	25.1	51.8
IAEDANS	A·S1	0.257	0.582	0.706	51.2	32.1	68.2
	A·S1·ADP	0.266	0.543	0.706	50.5	31.5	67.3
	A·S1·ADP·Vi	0.429	0.425	0.730	42.9	26.9	57.6

[a] Actin Cys374 was labeled with energy acceptor DABMI, and myosin SH1 was labeled with either MIANS or IAEDANS as energy donor. See Table 5 for experimental conditions.

fluorescence resonance energy and allow determinations of intermolecular distances from the two sites on S1 to Cys374 of actin in rigor actoS1. The energy transfer measurements also have yielded estimates of the distances in actoS1 liganded to MgADP and MgADP plus a phosphate analogue.

The properties of the AEDANS moiety linked to SH1 have been used in many previous studies to examine the nature of the SH1 site and in energy transfer studies involving this site. The labeling specificity of SH1 by IAEDANS also has been well documented. The ATPase activities of S1 labeled with IAEDANS in the absence of nucleotide confirm that the site of labeling is SH1. Less is known about the modification of SH1 by MIANS. The Ca^{2+}-ATPase of MIANS-labeled S1 is activated, but the enhancement is a factor of 2 lower than that of IAEDANS-labeled S1. The lower activity enhancement appears to be a characteristic of the probe and is not due to underlabeling of the site, or labeling of other sites.

The Ca^{2+}-ATPase activity of S1 singly labeled at SH2 by MIANS is unchanged, whereas the K^+/EDTA-ATPase activity is reduced by a factor of about 2. These results are in excellent agreement with the recent study of Hiratsuka (1992) and are very different from those observed with SH1-labeled S1 when the label is IAEDANS, FDNB, or NEM. The labeling of SH2 by IAEDANS has similar effects on the two types of ATPase activities as MIANS. While the quantitative effect of modification of a given thiol may be dependent upon the specific reagents, the structural effect resulting from the modification and propagation of the effect to the active site of S1 may be different for the two thiols. An examination of the emission properties of the probes each linked to the two sites may reveal differences in the reciprocal relationship between the active site conformation and the environments of the thiols.

With IAEDANS as the probe of the SH2 conformation, the binding of ADP at the active site has small effects on the emission spectrum. The binding of ADP and Vi shifts the probe to a slightly more polar environment (red spectral shift). Similar but more pronounced spectral changes are observed with MIANS as the probe. The binding of either ADP or ADP plus a phosphate analogue (either Vi or BeF) is accompanied by a substantial red spectral shift and a 2-fold decrease in the quantum yield of MIANS attached to SH2. These spectral changes could be due to movement of polar side chains of other residues to the SH2 environment or increased exposure of SH2 to the solvent. The latter interpretation is consistent with the recently reported increase in fluorescence quenching of MIANS at SH2 by acrylamide (Hiratsuka, 1992). The results from S1·ADP·Vi and S1·ADP·BeF suggest that the SH2 site should become exposed to a more polar environment during the steady-state hydrolysis of ATP. We have no spectral information on the initial S1·ATP complex prior to the catalytic step since rapid spectral scanning is needed to resolve the spectrum, but a large red spectral shift (12 nm) is observed during ATP hydrolysis. The size of the shift is similar to the shift detected upon addition of ADP plus a phosphate analogue. Upon depletion of ATP, the spectrum blue shifts by 4−5 nm to a position very similar to that for S1·ADP. The release of phosphate from the active site partially reverses the structural perturbation induced by ATP binding, but the reversal is not complete until ADP is removed from the active site. The quantum yield determined during hydrolysis is comparable to that for S1·ADP·Vi or S1·ADP·BeF. Release of phosphate at the end of hydrolysis increases the quantum yield toward the value observed for S1·ADP. These results can be interpreted in terms of a "closed" and an "open" conformation of the SH2 region. Before ATP binds to the active site, SH2 is in a "closed" or less open conformation in which (1) it is in a relatively nonpolar environment and (2) it is protected from interaction with the solvent. The binding of ATP converts the conformation of the SH2 region to an "open" conformation, bringing SH2 to a more polar environment and resulting in an increased exposure to the solvent. This increased exposure is maintained during the steady-state hydrolysis and reversed upon completion of

hydrolysis and release of products. While it is clear that the reversible conformational changes are modulated by structural changes that are initiated by ATP binding at the active site, it is not obvious as to what are the subsequent changes that can bring about the increased exposure of SH2. There are two simple mechanisms for this. One is reorientation and or movement of SH2 toward the surface of the protein as has been recently suggested (Hiratsuka, 1992). The other is nucleotide-induced reorientations of nonpolar side chains which surround SH2 in the absence of bound nucleotide. Such reorientations to expose SH2 need not require a movement of the thiol. The spectral results alone cannot discriminate between these two possibilities, and this point will be further discussed in conjunction with energy transfer data.

Formation of rigor actoS1 leads to a slightly more polar environment (red-shift) of SH2 with a small decrease in quantum yield. These changes are demonstrated by MIANS. Saturation of the active site of S1 in A·S1 with ADP or ADP plus Vi causes the SH2 environment to become less polar (4−10 nm blue-shift). The latter conformational changes are in the opposite direction of those for uncomplexed S1. During the steady-state hydrolysis of ATP, the MIANS emission spectrum red-shifts to a wavelength (434 nm) identical to that observed with uncomplexed S1 during hydrolysis. The blue-shifted spectrum observed at the end of hydrolysis reflects complete dissociation of P_i and the conformation of SH2 in A·S1·ADP. These spectral results suggest several different local conformations around the SH2 region dependent upon the biochemical state of myosin: (1) In uncomplexed myosin, SH2 shifts to a more polar environment when the active site is saturated by nucleotides, including ATP and its hydrolysis products. (2) In the weakly bound intermediate state A-M·ADP·P_i during the steady-state hydrolysis of ATP, the environment of SH2 becomes substantially more polar than in the strongly bound rigor state A·M. (3) Release of phosphate from the active site of myosin shifts SH2 in A·M·ADP to an environment that is less polar than that in A·M. These different conformations must be due to reorientations or movements of segments of the myosin heavy chain which are modulated by the active site conformations at different stages during ATP hydrolysis. As with uncomplexed S1, the observed spectral changes in A·S1 and A·S1·ADP·Vi cannot distinguish between movement of SH2 and reorientations of adjacent residues.

The microenvironment of SH1 in uncomplexed S1 is also considerably less polar than an aqueous environment. SH1 is likely in a slightly more polar environment than SH2 because the emission maximum of MIANS at SH1 is 4 nm longer than that at SH2. This difference in micropolarity between SH1 and SH2 is also supported by the spectral difference of AEDANS at the two sites. MIANS attached to SH1 senses perturbations by nucleotides and during ATP hydrolysis that are similar to those sensed by the same probe attached to SH2: nucleotides shift SH1 to a more polar environment. The extent of nucleotide-induced perturbations around SH1 appears to be less than that around the SH2 site in terms of spectral shifts, but the magnitude of the shifts alone does not necessarily reflect the extent of conformational perturbation. The SH1 site of S1 becomes slightly more polar in rigor A·S1 as is the SH2 site, as evidenced from a small red spectral shift and reduction in the quantum yield of the MIANS spectrum. The perturbations of the SH1 site in A·S1 induced by nucleotides appear to parallel those observed for the SH2 site, although the spectral changes are smaller at SH1. As a probe, IAEDANS appears less useful than MIANS in establishing a pattern of nucleotide-induced perturbations because of the smaller spectral changes. Nevertheless, the overall results from both probes are consistent with each other.

The fluorescence properties of the covalent adducts MIANS-*N*-Ac-Cys and AEDANS-*N*-Ac-Cys are similarly sensitive to medium polarity (Hiratsuka, 1992, 1993). Yet when attached to the same sites in S1, the spectrum of AEDANS-S1 is less sensitive to the effects of the binding of nucleotides and actin than MIANS-S1. IAEDANS has a flexible alkyl chain that links the protein site to the fluorescent anilinonaphthalene moiety. MIANS attached to a protein site does not have this motional freedom. The microenvironment that is sensed by AEDANS could be an assemble average which is different from that sensed by the rigid MIANS. The SH1 site has been previously studied by rigid probes such as IAF and ISAL (Agguire et al., 1986), and these probes also report large spectral changes in response to conformational changes initiated by the binding of nucleotides and actin. A rigid and small fluorescent sulfhydryl reagent (ABDF) was recently used to label SH1 (Hiratsuka, 1993). The attached ABD senses large spectral changes in the presence of ATP, but the changes are in the opposite direction of those sensed by MIANS reported here. ATP induces a 7-nm blue spectral shift and a 2-fold increase in the intensity of the ABD spectrum. On the other hand, the effect of formation of actoS1 with ABD-S1 on the spectrum is consistent with that reported by MIANS: a small decrease in quantum yield and little or negligible spectral shift. The fluorescent moiety in MIANS is the anilinonaphthalenesulfonate structure, whereas ABDF has a benzofurazan structure similar to the more familiar NBD fluoride. The anilinonaphthalenesulfonate and sulfamoylbenzofurazanyl moieties of the two probes attached to SH1 may have different orientations and interact differently with adjacent side chains. The apparent opposite changes of the SH1 microenvironment created by nucleotide binding may thus reflect the different properties of the two probes. To obtain a consistent view of the conformations and conformational changes around SH1 and SH2, it seems necessary to use the same probe as we have done here.

The penultimate Cys374 in rigor actoS1 is about equidistant from SH1 and SH2 [$R(^2/_3) \simeq 45$ Å], when determined with MIANS as the energy donor. The uncertainty due to random experimental errors is estimated to be <2.5 Å. An additional uncertainty in the calculated distances is in the value of the orientation factor, which cannot be experimentally determined and may be influenced by the localized conformation of the sites. The experimentally determined axial depolarizations of donor and acceptor provide a measure of the mobility of the transition dipoles and are useful in establishing to extent to which the assumption of random and rapid orientations ($\kappa^2 = {}^2/_3$) is valid. They also allow determination of the upper and lower limits of the orientation factor, and hence the maximum [R(max)] and minimum [R(min)] values of the donor−acceptor distance (Dale et al., 1979). The two distances have a common acceptor attached to actin Cys374, and this probe does not have a flexible structure. Its depolarization factor cannot be determined because it is nonfluorescent but must be the

same for both distances because the acceptor is located on the same site in actin. The experimentally determined axial depolarization factors for MIANS attached to SH1 and SH2 are essentially the same (Table 4), indicating very similar mobilities of the same donor probe at the two different sites. Thus, the experimental values of the two distances SH1−Cys374 and SH2−Cys374 in A·S1 reflect the separations between the sites rather than signficiant differences in probe orientations. This consideration supports the conclusion that, in actoS1, SH1 and SH2 are about equidistant from actin Cys374.

When determined with AEDANS as the energy donor, the Cys374−SH1 distance is about 4 Å longer than the Cys374−SH2 distance. The difference is beyond the estimated random error for energy transfer experiments. For any given separation, AEDANS also reports larger values than MIANS. Since the attached AEDANS is likely flexible as compared with the rigid structure of MIANS, the longer distances sensed by AEDANS may reflect this property of the probe. The mean value of the Cys374−SH1 distance obtained from the two different donor probes is 48.4 Å, and the mean value of the Cys374−SH2 distance is 45.9 Å. The difference (2.5 Å) is small enough to suggest that actin Cys374 is close to being equidistant from SH1 and SH2 in rigor actoS1. The present value of $R(^2/_3)$ for the Cys374−SH1 distance in rigor A·S1 is in good agreement with previous reports using IAEDANS and IAF as the donor−acceptor pair (Takahasi, 1979; Trayer & Trayer, 1983; Arata, 1986).

While the distances across rigor A·S1 can be determined in a straightforward manner, the determination of the same distances in A·S1·ADP and A·S1·ADP·Vi requires corrections for contribution of donor signal from other donor-containing species. The corrections were made using appropriate published equilibrium constants for Schemes 1 and 2. Since both S1 and actin used in the present study were alkylated at either SH1 or SH2 of S1 and at actin Cys374, the appropriate constants are those obtained with similarly alkylated proteins. Some of the constants used were obtained with S1 alkylated at SH1 and others with actin alkylated at Cys374. While the precise value of a given constant may be dependent upon which protein is alkylated, the difference may not be very large. For example, the value of K_4 obtained with S1 alkylated at SH1 (Lin et al., 1993) is within a factor of 2 of the value obtained with alkylated actin (Criddle et al., 1985), and this difference has very little effect on the estimated error in the calculated distance.

It is clear from the present data that the Cys374−SH2 distance is not sensitive to ligands and not affected by the biochemical state of actoS1, regardless of whether the donor is MIANS or AEDANS. On the other hand, the Cys374−SH1 distance [$R(^2/_3)$] is reduced by 7−8 Å when A·S1 is incorporated into the A·S1·ADP·Vi complex. Decreases of comparable magnitudes are also found in R(min) and R(max). The decrease in R is detected by both donor probes located at the SH1 site and is due to the presence of both bound ADP and Vi at the S1 active site. Bound ADP alone has little or no significant effect on the distance, consistent with a previous result (Trayer & Trayer, 1983). The large decrease in R is a consequence of a near 2-fold increase in transfer efficiency. Because the transfer efficiency is determined by both the donor−acceptor separation and the relative orientation of probe dipoles, the observed increased transfer efficiency could be due to a change in κ^2 rather than a change in donor-acceptor separation. A 2.8-fold increase in κ^2 in A·S1·ADP·Vi could account for the observed increase in E without invoking a change in R. A change in κ^2 of this magnitude would be reflected in the measured mobility of the donors. No significant differences are observed in donor anisotropy among the states S1, S1·ADP, and S1·ADP·Vi. The present data cannot distinguish between the intermediate case in which both κ^2 and R change and the case in which κ^2 is unaltered. In the absence of additional information, the 2-fold increase in energy transfer is interpreted in terms of a significant decrease in the Cys374−SH1 distance in A·S1·ADP·Vi. This result suggests that during the steady-state ATP hydrolysis or in the weak-binding state (A·S1·ATP or A·S1·ADP·Pi) SH1 of S1 and actin Cys374 become closer to each other in actoS1.

Arata reported the separation between Cys374 and SH1 in A·S1 cross-linked by 1-ethyl-3-(dimethylaminopropyl)-carbodiimide (EDC) in the absence and presence of ATP (1986). He obtained essentially identical distances (46−47 Å) for uncross-linked rigor A·S1, A·S1 cross-linked in the absence of nucleotide and in the presence of ADP or AMPPNP. These results, which were obtained with the IAEDANS/IAF donor−acceptor pair, are in agreement with the present results obtained with MIANS as the donor attached to SH1. It appears that covalent cross-linking by EDC in the absence of ATP has no effect on the conformation of actoS1. However, for A·S1 cross-linked in the presence of ATP the distance was 6−8 Å longer (52−55 Å) than rigor A·S1. This longer distance has been attributed to the presence of trapped ATP at the S1 active site, although AMPPNP trapped at the active site by the same cross-linking has no detectable effect on the distance. Both cross-linked A·S1 containing trapped ATP and the preparation A·S1·ADP·Vi used in the present work are considered stable analogues of actoS1 in the weak-binding state with a similar overall conformation. Yet the observed nucleotide-induced changes of the intersite distance across the binary protein complex of the two preparations are in the opposite directions. This raises the question of whether the two preparations are conformationally equivalent. In the absence of ATP, the cross-linking reaction involves the amino-terminal acidic residues of actin and either the 50-kDa or the 20-kDa tryptic segment of S1 heavy chain (Monet et al., 1981; Sutoh, 1983). The recent model for rigor A·S1 (Rayment et al., 1993b) suggests at least two main contact regions between actin and S1: (1) an ionic interaction between the NH_2-terminal segment of actin with the S1 segment between residues 624 and 647 (the 50-kDa segment/20-kDa segment junction) which have been implicated from cross-linking studies, and (2) a stereospecific interaction involving hydrophobic residues which include the segment of S1 from amino acids 529−553 located on the 50-kDa segment. It cannot be predicted how these contact regions may shift in the presence of trapped ATP, and the possibility exists that different segments of the two proteins are cross-linked dependent upon the absence or presence of trapped ATP. It is not clear to what extent cross-linking itself may influence the observed increase in the Cys374−SH1 distance.

The observations of a decrease in the Cys374−SH1 distance and no change in the Cys374−SH2 distance when rigor A·S1 is converted to A·S1·ADP·Vi provide an assessment of the relative mobility of the two thiols. In a recent FRET study, Miki (1991) showed that the small subdomain

of actin monomer is rigid. The rigidity of the subdomain which contains the sites for myosin is preserved in polymerized actin and in the presence of S1. This conclusion is based on the observation that the distance between Tyr69 and Cys374 in actin determined in a variety of conditions (e.g., G-actin, F-actin, regulated F-actin ± Ca^{2+}, F-actin+S1) is within the narrow range of 21−23 Å. If the actin structure in A·S1 is rigid as these FRET results suggest, the position of Cys374 of actin may be assumed to be fixed in A·S1. Thus, the 7−8 A decrease in the Cys374−SH1 distance suggests a movement of SH1 toward the actin site. Since the Cys374−SH2 distance is not sensitive to the presence of ADP + Vi, SH2 appears to be motionless with respect to the actin site, regardless of the biochemical state of A·S1.

Previous reports have shown that SH1 and SH2, in the presence of nucleotides, can move toward each other to within 4−5 Å. This information comes from a variety of studies including cross-linking (Reisler et al., 1974; Burke & Reisler, 1977; Wells & Yount, 1979; Huston et al., 1988) and FRET. FRET studies reported a decrease of the SH1−SH2 distance by 7−10 Å upon addition of MgADP (Dalbey et al., 1983; Cheung et al., 1985), AMPPNP (Dalbey et al., 1983), and MgADP + Vi (Cheung et al., 1991). The distance decrease was shown to occur in two kinetic steps (Garland et al., 1988), and the flexible nature of the SH1−SH2 segment was also demonstrated by FRET data (Cheung et al., 1991). Other fluorescence studies have suggested that actin binding to S1 induces relative movements of the 25-kDa segment and the SH1 region of the 20-kDa segment, and this movement is reversed when ADP binds to A·S1 (Lin & Cheung, 1991). A recent study of the intramolecular cross-linking between the 25- and 20-kDa segments has corroborated this suggestion and directly demonstrated the reciprocal effect of actin and ADP on the relative movement of the two segments (Bertrand et al., 1992). These movements of S1 segments induced by actin and substrate binding have been regarded as a means of communication between different parts of S1 and the basis of structural dynamics of the actomyosin·nucleotide system. In the case of the two sulfhydryl groups SH1 and SH2, a recurrent question is whether both thiols are mobile or only one is mobile and the other is stationary. Several reports have suggested that SH2 is mobile and SH1 is relatively immobile. Kasprzak et al. (1989) showed that MgATP had a very small effect on the FRET distance between SH1 and an antipeptide bound to the segment of residues 633−642 of S1 heavy chain, but a larger effect on the distance between SH2 and bound antipeptide. From photo-cross-linking results, Rajasekharan et al. (1989) observed ATP-induced displacement of SH2 relative to the 50-kDa segment of S1 heavy chain. These results are consistent with the notion that SH2 is mobile and SH1 is stationary, in contrast to the conclusions reached in the present work. Hiratsuka has recently suggested in separate studies that both SH2 (Hiratsuka, 1992) and SH1 (Hiratsuka, 1993) can move. His conclusion of movement of SH2 is based on the observation of nucleotide-induced red spectral shifts of the fluorescence emission spectrum of MIANS attached to this site. We have observed similar spectral shifts, but the shifts alone do not necessarily reflect movement of the probe to the surface. Resolution of this issue must await detailed crystallographic information including positions of the side chains of nucleotide-bound S1. In the absence of such information, we attempted to obtain an insight on the possible conformation around the SH1−SH2 segment from a crude model built from the C^{α} coordinates of the S1 structure (Rayment et al., 1993a) and energy minimization of incorporated side chains. The model suggested that SH2 is located within a hydrophobic cage formed by Ala585, Phe467, and Ile469. The sulfur atom of SH2 is almost in van der Waals contacts with the side chains of the three surrounding residues. This conformation would explain the inaccessibility of SH2 toward alkylating reagents. Rotation of Ile469 side chain could create a relatively large opening toward the solvent. If such a perturbation could be caused by the binding of ATP or ADP + Vi, SH2 would find itself in a less hydrophobic microenvironment without any movement of its own. This could explain the observed large red spectral shift of MIANS attached to SH2 in the presence of either ADP or ADP + Vi. The model also suggested that SH1 would be accessible to solvent perturbation as there appeared to be a narrow cavity leading to SH1 with no apparent blockage. The crystal structure of S1 (Rayment et al., 1993a) shows that SH2 (Cys697) and SH1 (Cys707) are located on two different helices which are separated by Gly699 and are oriented at an angle of greater 110° with respect to each other. Gly699 may provide a flexible hinge allowing independent reorientations of the two helices. By triangulation of the three sites SH1, SH2, and actin Cys374 with SH2 and Cys374 being stationary, a movement of SH1 toward SH2 by 7−8 Å can easily bring SH1 closer to actin Cys374 in actoS1. This movement of SH1 within the motor domain of myosin may in turn induce movements of other segments to bring about the ATP-induced lateral movement of the C-terminal segment of the heavy chain recently proposed for the actoS1 complex (Rayment et al., 1993b).

ACKNOWLEDGMENT

We thank Dr. Ivan Rayment for providing the C^{α} coordinates of the X-ray structure of S1 prior to deposit in the data bank. We also thank Dr. Chi-hao Luan for assistance in building a crude model for the structure of myosin S1 and Mr. Mingda She in the calculations of equilibrium concentrations of actomyosin in the presence of ligands.

REFERENCES

Aguirre, R., Gonsoulin, F., & Cheung, H. C. (1986) *Biochemistry 25*, 6827−6835.

Aguirre, R., Lin, S.-H., Gonsoulin, F., Wang, C.-K., & Cheung, H. C. (1989) *Biochemistry 28*, 799−809.

Arata, T. (1986) *J. Mol. Biol. 191*, 107−116.

Bertrand, R., Derancourt, J., & Kassab, R. (1992) *Biochemistry 31*, 12219−12226.

Bhandari, D. G., Trayler, H. R., & Trayler, I. P. (1985) *FEBS Lett. 187*, 160−166.

Botts, J., Thomason, F., & Morales, M. F. (1989) *Proc. Natl. Acad. Sci. U.S.A. 86*, 2204−2208.

Burke, M., & Reisler, E. (1977) *Biochemistry 16*, 5559−5563.

Cheung, H. C., Garland, F., & Gonsoulin, F. (1983) *J. Biol. Chem. 258*, 5775−5786.

Cheung, H. C. (1991) in *Topics in Fluorescence Spectroscopy* (Lakowicz, J. R., Ed.) Vol. 2, pp 127−176, Plenum Press, New York.

Cheung, H. C., Garland, F., & Gonsoulin, F. (1985) *Biochim. Biophys. Acta 832*, 52−62.

Cheung, H. C., Gryczynski, I., Malak, H., Wiczk, W., Johnson, M. L., & Lakowicz, J. R. (1991) *Biophys. Chem. 40*, 1−17.

Criddle, A. H., Geeves, M. A., & Jeffries, T. (1985) *Biochem. J. 232*, 343−349.
Dalbey, R. E., Weiel, J., & Yount, R. C. (1983) *Biochemistry 22*, 4696−4706.
Dale, R. E., Eisinger, J., & Blumberg, W. E. (1979) *Biophys. J. 26*, 161−193.
Eisenberg, E., & Greene, L. (1980) *Annu. Rev. Physiol 42*, 293−309.
Eisenberg, E., & Hill, T. (1985) *Science 277*, 999−1006.
Fiske, C. H., & SubbaRow, Y. (1925) *J. Biol. Chem. 66*, 375−400.
Garland, F., Gonsoulin, F., & Cheung, H. C. (1988) *J. Biol. Chem. 263*, 11621−11623.
Geeves, M. A. (1989) *Biochemistry 28*, 5864−5871.
Geeves, M. A., Goody, R. S., & Gutfreund, H. (1984) *J. Muscle Res. Cell Motil. 5*, 351−361.
Goodno, C. C. (1979) *Proc. Natl. Acad. Sci. U.S.A. 76*, 2620−2624.
Grinvald, A., & Steinberg, I. Z. (1974) *Anal. Biochem. 59*, 583−598.
Hiratsuka, T. (1992) *J. Biol. Chem. 267*, 14941−14948.
Hiratsuka, T. (1993) *J. Biol. Chem. 268*, 24742−24750.
Houk, T. W., & Ue, K. (1974) *Anal. Biochem. 62*, 66−74.
Huston, E. E., Grammer, R. G., & Yount, R. G. (1988) *Biochemistry 27*, 8945−8952.
Kasprazk, A. A., Chaussepied, P., & Morales, M. F. (1989) *Biochemistry 28*, 9230−9238.
Lin, S.-H., & Cheung, H. C. (1991) *Biochemistry 30*, 4317−4322.
Lin, S.-H., Hazelrig, J. B., & Cheung, H. C. (1993) *Biophys. J. 65*, 1433−1444.
Miki, M. (1991) *Biochemistry 30*, 10878−10884.
Miki, M., Barden, J. A., Hambly, B. D., & dos Remedios, C. G. (1986) *Biochem. Int. 12*, 725−731.
Monet, D., Bertrand, R., Pantel, P., Audemard, E., & Kassab, R. (1981) *Biochemistry 20*, 2110−2120.
Monet, D., Bonet, A., Audemard, E., & Bonicle, J. (1989) *J. Muscle Res. Cell Motil. 10*, 10−24.
Parker, C. A., & Reese, W. T. (1960) *Analytst (London) 58*, 587−598.
Phan, B., & Reisler, E. (1992) *Biochemistry 31*, 4787−4793.
Phan, B. C., Faller, L. D., & Reisler, E. (1993) *Biochemistry 32*, 7712−7719.
Rajasekharan, K. N., Mayadevi, M., & Burke, M. (1989) *J. Biol. Chem. 264*, 10810−10819.
Rayment, I., Rypniewski, W. R., Schmidt-Bäse, K., Smith, R., Tomchick, D. R., Benning, M. W., Winkelmann, D. A., Wesenberg, G., & Holden, H. M. (1993a) *Science 261*, 50−58.
Rayment, I., Holden, H. M., Whittaker, M., Yohn, C. B., Lorenz, M., Holmes, K. C., & Milligan, R. A. (1993b) *Science 261*, 58−65.
Reisler, E. (1982) *Methods Enzymol. 85*, 84−93.
Reisler, E., Burke, M., & Harrington, W. F. (1974a) *Biochemistry 13*, 2014−2022.
Reisler, E., Burke, M., Himmelfarb, S., & Harrington, W. F. (1974b) *Biochemistry 13*, 3877−3840.
Scott, T. A., Spencer, R. D., Leonard, N. J., & Weber, G. (1970) *J. Am. Chem. Soc. 92*, 697−695.
Smith, S. J., & Eisenberg, E. (1990) *Eur. J. Biochem. 193*, 69−73.
Spudich, J. A., & Watt, S. (1971) *J. Biol. Chem. 246*, 4866−4871.
Sutoh, K. (1983) *Biochemistry 22*, 1579−1585.
Takashi, R. (1979) *Biochemistry 18*, 5164−5169.
Trayer, H. R., & Trayer, I. P. (1983) *Eur. J. Biochem. 135*, 47−59.
Wagner, P. D., & Weeds, A. G. (1977) *J. Mol. Biol. 109*, 455−473.
Wang, C.-K., & Cheung, H. C. (1986) *J. Mol. Biol. 191*, 509−521.
Weeds, A. G., & Taylor, R. S. (1975) *Nature 257*, 54−56.
Wells, C., & Yount, R. G. (1982) *Methods Enzymol. 85*, 93−116.
Wells, C., & Bagshaw, C. R. (1984) *J. Muscle Res. Cell Motil. 5*, 97−112.

BI950177J